

# DuDoUniNeXt: Dual-domain unified hybrid model for single and multi-contrast undersampled MRI reconstruction

Ziqi Gao<sup>1,2</sup>, Yue Zhang<sup>1,2</sup>, Xinwen Liu<sup>3</sup>, Kaiyan Li<sup>1,2</sup>, and S. Kevin Zhou<sup>1,2</sup>

<sup>1</sup> School of Biomedical Engineering, Division of Life Sciences and Medicine, University of Science and Technology of China, Hefei, Anhui, China 230026

<sup>2</sup> Center for Medical Imaging, Robotics, Analytic Computing & Learning (MIRACLE), Suzhou Institute for Advance Research, University of Science and Technology of China, Suzhou, Jiangsu, China 215123

<sup>3</sup> School of Electrical Engineering and Computer Science, The University of Queensland

**Abstract.** Multi-contrast (MC) Magnetic Resonance Imaging (MRI) reconstruction aims to incorporate a reference image of auxiliary modality to guide the reconstruction process of the target modality. Known MC reconstruction methods perform well with a fully sampled reference image, but usually exhibit inferior performance, compared to single-contrast (SC) methods, when the reference image is missing or of low quality. To address this issue, we propose DuDoUniNeXt, a unified dual-domain MRI reconstruction network that can accommodate to scenarios involving absent, low-quality, and high-quality reference images. DuDoUniNeXt adopts a hybrid backbone that combines CNN and ViT, enabling specific adjustment of image domain and k-space reconstruction. Specifically, an adaptive coarse-to-fine feature fusion module (AdaC2F) is devised to dynamically process the information from reference images of varying qualities. Besides, a partially shared shallow feature extractor (PaSS) is proposed, which uses shared and distinct parameters to handle consistent and discrepancy information among contrasts. Experimental results demonstrate that the proposed model surpasses state-of-the-art SC and MC models significantly. Ablation studies show the effectiveness of the proposed hybrid backbone, AdaC2F, PaSS, and the dual-domain unified learning scheme.

**Keywords:** Unified model · Undersampled MRI reconstruction · Multi-contrast MRI · Hybrid model

## 1 Introduction

Magnetic resonance imaging (MRI) is a superior imaging technique that provides multiple sequences of different modalities for comprehensive disease diagnosis. However, MRI typically involves long scanning time and expensive acquisition costs, which impose a heavy burden on patients. Mainstream meth-

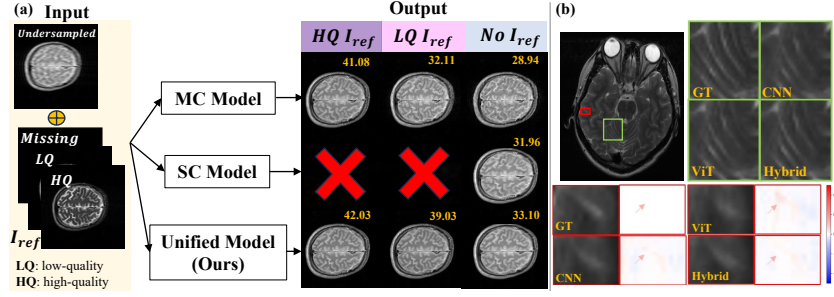


**Fig. 1.** The main idea of DuDoUniNeXt. (a) The reconstruction results of different models with absent, an LQ, or an HQ auxiliary image. The upper part shows the results of the MC model, the middle part shows the results of the SC model, and the bottom is the results of the proposed DuDoUniNeXt. The PSNR values (dB) of the reconstructed images are shown in the upper right corners. (b) The reconstruction emphasis of CNN, ViT, and our hybrid backbone. The green and red boxes highlight two typical patterns: highly structured lines and isolated fine details.

ods for accelerating MRI can be categorized into *single-contrast (SC) methods* [3,6,10,11,34,38,32,33,41,21,17,4,15,20,29,9] that reconstruct MRI from undersampled data of a single modality, and *multi-contrast (MC) methods* [5,7,23,30,43,37,35,13] that utilize auxiliary easy-to-obtain modalities to assist in the reconstruction process of the target modality. Owing to the use of auxiliary information, MC methods usually achieve superior reconstruction quality.

Generally, MC reconstruction networks assume the reference image of auxiliary modality is fully sampled and of high quality [24,26,36,42,43]. These networks reconstruct the undersampled images by effectively integrating complementary information from the reference image. RsGAN [5] extends the adaptability towards a slightly downsampled ( $2\text{-}3\times$ ) reference image. Although MC methods exhibit enhanced reconstruction quality, they inevitably fail in real-life scenarios where the reference images are missing or of low quality (e.g., undersampled). For example, Fig. 1 (a) shows the reconstruction results of SC model and MC model with three types of reference images: missing, low-quality (LQ), or high-quality (HQ). Note that the MC model is MC-DuDoRNet from [43] and the SC model is SC-DuDoRNet [43]. It is observed that the MC model works well with an HQ auxiliary image (41.08dB in PSNR), but its performance degrades significantly with an LQ (32.11dB) or missing auxiliary image (28.94dB). In contrast, the SC model shows acceptable reconstruction performance (31.96 dB), however, it lacks the flexibility to incorporate HQ or LQ reference images for further performance enhancement.

To solve the aforementioned issues, we propose a dual-domain unified dynamic hybrid model, dubbed DuDoUniNeXt, for both single- and multi-contrast undersampled MRI reconstruction. Our DuDoUniNeXt can adaptively incorporate reference images of various qualities, and outperforms both MC and SC models (see Fig. 1 (a)). The followings are our key contributions:

- **The first dual-domain unified network for both SC and MC MRI reconstruction.** DuDoUniNeXt is a novel dual-domain unified learning network that supports undersampled MRI reconstruction with high-quality, low-quality, or missing auxiliary images. The unified model has fewer parameters than the combination of two single-purpose models.
- **Contrast-aware dynamic encoder for MC MRI reconstruction.** Our encoder utilizes both complementary and consistent information from MC MRI concurrently with a Partially Shared Shallow feature extractor (PaSS) and supports dynamic MRI inputs with an Adaptive Coarse-to-Fine feature enhancement module (AdaC2F).
- **Dual-domain CNN-ViT hybrid backbone for MRI reconstruction.** The CNN-ViT hybrid backbone used by DuDoUniNeXt supports domain-specific model building combined with human heuristics, which surpasses unitary CNN or ViT backbones’ efficacy with high efficiency (Fig. 1 (b)).
- **Demonstrated robustness and effectiveness.** DuDoUniNeXt surpasses several popular single-contrast undersampled MRI reconstruction models on FastMRI and outperforms popular multi-contrast models on IXI considering multiple target-reference combinations.

## 2 Method

In this paper, we propose DuDoUniNeXt for unified SC and MC MRI reconstruction. DuDoUniNeXt takes a dual-domain unified learning framework (Sec. 2.1) consisting of recurrent k-space and image recovery networks. The reference image is injected into the image recovery network in each recurrent block with a contrast-aware dynamic encoder (Sec. 2.2). The backbone is an efficient CNN-ViT hybrid backbone that supports domain-specific adjustment (Sec. 2.3).

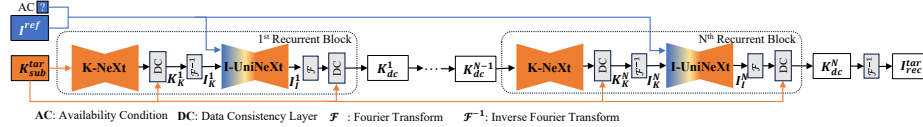


**Fig. 2.** The overall dual-domain unified learning framework. Each recurrent block contains one network for single-contrast k-space restoration, K-NeXt, and one network for unified image restoration, I-UniNeXt, with two interleaved DCs. Availability condition (AC) keeps I-UniNeXt notified for different conditions of  $I_{ref}$ .

### 2.1 Dual-domain Unified Learning Framework

Given a missing, LQ, or HQ reference modality  $I_{ref}^{ref} \in \mathbb{C}^{hw}$ , a corresponding availability condition (AC) in  $\{0,1\}$  (with 0 denoting missing  $I_{ref}^{ref}$  and 1 denoting available  $I_{ref}^{ref}$ ), and undersampled k-space of the target modality  $K_{sub}^{tar} \in \mathbb{C}^{hw}$ , DuDoUniNeXt aims to reconstruct the target image  $I_{rec}^{tar} \in \mathbb{C}^{hw}$ . As outlined

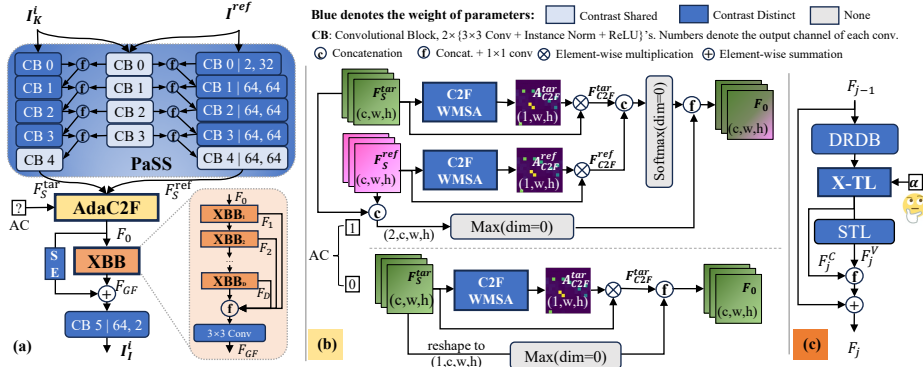


**Fig. 3.** The architecture of I-UniNeXt. Panel (a) shows the overall architecture of I-UniNeXt, with the detailed architecture of the PaSS illustrated in the blue box and XBB illustrated in the orange box. (b) and (c) show the dedicated structure of AdaC2F and the domain-specific Hybrid Block ( $\text{XBB}_j$ ), respectively.

in Fig. 2, DuDoUniNeXt uses recurrent learning with data consistency (DC) layers [31,33] for iterative feature recovery and adopts dual-domain learning [43] to utilize the synergy of image and k-space domain learning. The overall framework contains  $N$  Recurrent Blocks, each of which performs one round of K-space (K-NeXt) and image-domain (I-UniNeXt) recovery on the input data.

Different from the existing dual-domain networks, DuDoUniNeXt uses a different image and k-space layout and reference modality injection approach to achieve unified learning. In the  $i^{\text{th}}$  ( $i \in 1, \dots, N$ ) recurrent block, an estimation of the target modality is first given by a single-contrast k-space recovery network, K-NeXt. The input of K-NeXt is  $K_{sub}^{tar}$  for the  $1_{st}$  block and  $K_{dc}^{i-1}$ , the output of the previous recurrent block, for the others. K-NeXt’s output that is enforced data consistency is  $K_K^i$  and  $I_K^i = \mathcal{F}^{-1}(K_K^i)$ .  $I_K^i$ , together with the reference image  $I_{ref}$  and AC, are sent to a unified multi-contrast image recovery network, I-UniNeXt.  $K_{dc}^i$  is the output of I-UniNeXt after data consistency operation. The final output of DuDoUniNeXt is given by  $I_{rec}^{tar} = \mathcal{F}^{-1}(K_{dc}^N)$ . The overall loss function is the summation of dual-domain  $L_2$  loss of each recurrent block:

$$L = \sum_{i=1}^N (\|K_{GT}^{tar} - K_K^i\|_2 + \|I_{GT}^{tar} - \mathcal{F}^{-1}(K_{dc}^i)\|_2), \quad (1)$$

in which  $K_{GT}^{tar}$  and  $I_{GT}^{tar}$  are the ground truth of the target K-space and image.

Intuitively, our DuDoUniNeXt can utilize the bias towards low-frequency in K-space learning with  $L_2$  loss [27] to give a rough estimation with K-NeXt and dynamically incorporate a reference to improve image details with I-UniNeXt.

## 2.2 Contrast-aware Dynamic Encoder

The key to the unified reconstruction model lies in how to leverage reference images of varying qualities, which is supported by the contrast-aware dynamic

encoder in I-UniNeXt. Specifically, the encoder contains two core components: the Partially Shared Shallow feature extractor (PaSS) and Adaptive Coarse-to-Fine feature enhancement (AdaC2F).

**Partially Shared Shallow Feature Extractor** The target and reference images share the same anatomical structure and visualize soft tissue differently. To process both complementary and consistent information conveyed by multi-contrast inputs simultaneously, we propose PaSS to extract the multi-contrast shallow features with distinct and shared encoders, respectively. As depicted in Fig. 3(a), PaSS consists of a shared branch and two modality-specific branches that have the same layer-wise convolution structure. For each modality, the consistent anatomical information captured by the shared branch is emphasized in the specific branches by layer-wise feature concatenation and  $1 \times 1$  convolution. Two specific branches share the last convolution block (CB4) for memory efficiency and output modality-specific shallow features  $F_S^{tar}$  and  $F_S^{ref}$  respectively. The rationale behind it is the commonality of high-level information in MC MRI.

**Adaptive Coarse-to-fine Feature Enhancement** The Max function is typically applied for multi-modal fusion [2], yet prone to detail loss and of limited ability to cope with the variance in the input’s quality. To support both self and reference-enhancement for  $F_S^{tar}$  and  $F_S^{ref}$  adaptively, we propose AdaC2F that combines Max with multi-head self-attention (MSA) enhanced features reweighed by Softmax into a fused feature map  $F_0$ . We depict the variants of AdaC2F with different ACs in Figure 3(b). The Softmax operates on the feature map enhanced by modality-specific coarse-to-fine windowed MSA (C2F-WMSA). Compared to the convolutional attention mechanism built on inductive bias, MSA is a data-specific operation [28] with a large receptive field, enabling adaptively removing global artifacts. Considering that MSA has weaker detail preserving ability (Fig. 1(b)), we compile two WMSAs with window sizes equal to  $(16 \times 16)$  and  $(8 \times 8)$  to produce modality-specific attention map  $A_{C2F}^*$  that captures the global structure and emphasize the dedicated details:

$$F_{C2F}^* = F_S^* \odot A_{C2F}^*, A_{C2F}^* = \mathbf{WMSA}_8(\mathbf{WMSA}_{16}(F_S^*)), \quad (2)$$

where  $\odot$  is the Hadamard product and  $*$  can be the target or reference branch.

### 2.3 Domain-specific CNN-ViT hybrid backbone

ViTs are more performant for undersampled MRI reconstruction than the CNN counterparts [42,16,26] at the cost of training difficulty and heavy computation. Also, ViT-based models typically have weaker detail preservation ability (Fig. 1(b), red boxes). To balance between efficiency and efficacy, we propose a novel CNN-ViT hybrid backbone, XBB, consisting of D domain-specific hybrid blocks and a conventional global feature fusion operation as [43], shown in Fig. 3(a), the orange part. The design of each XBB is shown in Fig. 3(c). It is constructed by vertically stacking a Dilated Residual Dense Block (DRDB) [8] and a Swin Transformer Layer (STL) [22,16,25] followed by a  $1 \times 1$  convolution operation that supports the hybrid interaction of CNN features  $F_j^C$  and ViT features  $F_j^V$ . Intuitively, XBB utilizes the complementary properties of CNN (detail preservation) and ViT (feature aggregation) through this specific vertical layout design.

Another key property of XBB is that it can serve to build domain-specific models by adjusting the transition layer (X-TL). X-TL is a  $1 \times 1$  convolution that compresses  $c$  feature maps into  $\lfloor \alpha c \rfloor$ , where  $\alpha \in (0, 1]$  is adjustable. Under a budget of total parameters, a larger  $\alpha$  means more parameters for the ViT part and a smaller portion for CNN. This helps to build a domain-specific model by combining human heuristics: image restoration is considered a local problem [22] so it may benefit from a smaller  $\alpha_I$  while K-space shows a global dependency in recent K-space interpolation work [27,8]; thus a larger  $\alpha_K$  may help.

To further improve target contrast recovery, the globally fused feature  $F_{GF}$  is combined with a global residual connection of a target-specific feature map enhanced by Squeeze-and-Excitation (SE) [14]. Feature is later passed through several convolutional layers, CB5, to generate the reconstruction output  $I_I^i$ :

$$I_I^i = \mathbf{SE}(F_0) + \mathbf{CB5}(F_{GF}), F_{GF} = \mathbf{Conv}(\mathbf{Concat}(F_1, \dots, F_D)). \quad (3)$$

K-NeXt is a SC k-space recovery network consisting of XBB and CB5 only.

## 2.4 Training scheme

We employ a simple yet effective training strategy: exposing the network to various input configurations by providing HQ, LQ, and absent reference images randomly with equal probabilities of  $(\frac{1}{3}, \frac{1}{3}, \frac{1}{3})$ . Although we do witness an improvement by duplicating  $I_{tar}^{sub}$  as input when  $I_{ref}$  is missing, we use black images for simplified idea demonstration and controlled experiments.

## 3 Experiment

**Setup** In this section, we present the experimental setup including details of the dataset, implementation, and evaluation.

**Dataset** We use one simulation dataset, the Multi-contrast IXI brain dataset[1], and one dataset containing raw coil-combined k-space, the FastMRI knee[19,39] dataset. We use the well-aligned T<sub>2</sub>- and PD-weighted coil-combined magnitude-only slices from 576 overlapped subjects in IXI and raw k-space coronal PD-weighted slices from 1,172 subjects with or without fat suppression in FastMRI. We follow the same pre-processing and dataset partition conventions as those in [42] and [4,19], respectively. Our model, together with all other supervised models, is trained with 1D Cartesian sampling trajectories with a fixed portion (12.5%) of the auto-calibration region, and the acceleration rates ranging from 4 to  $8 \times$  randomly and uniformly.

**Implementation** We implement our method in PyTorch using an NVIDIA GeForce RTX 3090 GPU with 24GB memory. The Adam solver [18] is used to optimize DuDoUniNeXt with  $lr = 0.0001$ ,  $\beta_1\beta_2 = 0.5, 0.999$ . The training batch size is 1. I-UniNeXt and K-NeXt share the parameters among all recurrent blocks. In the main experiments, we simply use a moderate  $\alpha_K = \alpha_I = 0.5$ ; yet we do recognize performance gain by adjusting the rate (Table 2 in the supplementary).

PSNR(dB)/SSIM(%)		FastMRI		Multi-contrast IXI			
Acc. rate		4x	8x	4x	8x	4x	8x
SC reconstruction: target		PD knee		T2w brain		PD brain	
SC Models	Zero Filling	28.82/85.12	28.20/83.23	24.85/77.40	23.93/77.30	24.68/86.73	23.78/77.00
	UNet	30.71/88.99	29.18/85.63	27.76/87.97	24.54/85.38	27.67/87.59	24.13/85.27
	DiffuseRecon	31.38/82.05	29.51/76.23	N/A	N/A	N/A	N/A
	Score-MRI	30.33/87.39	28.81/84.23	28.78/93.69	24.72/89.48	28.64/87.59	24.74/85.27
	D5C5	33.13/86.30	30.31/86.30	31.36/95.56	27.34/91.05	31.75/95.58	27.80/91.87
	SC-DuDoRNet	33.77/91.63	31.12/87.78	32.94/96.57	28.50/92.75	33.61/96.64	29.25/93.51
	SC-Dual Hybrid	<b>33.91/91.78</b>	<b>31.18/87.91</b>	33.65/97.01	28.67/93.07	34.26/97.04	29.57/93.89
MC Models	Without $I_{ref}$						
	MTrans	-	-	27.16/86.34	25.92/85.92	27.34/86.13	26.01/85.50
	MC-DuDoRNet	-	-	28.01/90.79	26.27/88.23	28.62/91.19	26.71/89.22
	Ours	-	-	<b>34.14/97.27</b>	<b>28.91/93.46</b>	<b>34.56/97.30</b>	<b>29.62/94.23</b>
MC recon.: ref. & tar.				ref:PD, tar:T2w		ref:T2w, tar:PD	
MC Models	With a LQ ( $2\times$ under-sampled) $I_{ref}$						
	MTrans	-	-	27.71/88.31	26.45/88.06	31.57/94.61	30.33/94.57
	MC-DuDoRNet	-	-	29.80/90.37	27.96/88.19	31.35/92.02	29.56/90.42
	Ours	-	-	<b>37.97/98.73</b>	<b>35.66/98.21</b>	<b>38.74/98.83</b>	<b>36.38/98.35</b>
	With a HQ (fully-sampled) $I_{ref}$						
	MTrans	-	-	36.62/98.01	35.16/97.84	37.49/98.25	36.16/98.14
	MC-DuDoRNet	-	-	39.63/99.02	37.55/98.60	40.14/99.09	37.83/98.67
	Ours	-	-	<b>40.22/99.12</b>	<b>37.81/98.72</b>	<b>40.74/99.18</b>	<b>38.44/98.83</b>

**Table 1.** Quantitative comparisons on the reconstruction of brain and knee images under acceleration rates of  $4\times$  and  $8\times$ . The **best** results are colored in **red**.

Evaluation For comparison, we use the official implementations of D5C5 [33], UNet [19], DiffuseRecon [29], Score-MRI [4], DuDoRNet [43], and MTrans [7]. We use the provided checkpoints trained on the same FastMRI dataset for the two diffusion models [29, 4] and train the rest models following their default settings unless otherwise noted. In Table 1 of the supplementary, we list a modified subset of hyper-parameters in DuDoRNet and MTrans to regulate the total parameters of single-purpose SoTA models. The final evaluation is performed on 5,145 slices of PD knee, 700 slices of T2w, and 700 slices of PD brain from unseen subjects during training. We use the Peak Signal-to-Noise Ratio (PSNR) and Structural Similarity Index (SSIM) to evaluate the reconstruction ability.

**Main results** Quantitative evaluations on FastMRI and IXI are summarized in Table 1. The first sub-table validates the SC reconstruction ability of various methods on two datasets. On the one hand, by substituting the backbone of SC-DuDoRNet with our hybrid backbone, SC-Dual Hybrid improves the performance consistently for both datasets. On the other hand, our unified model, DuDoUniNeXt, surpasses the SC models with 0.4-1.2dB in PSNR. For comparison, other MC models have inferior performance when  $I_{ref}$  is missing. For example, MC-DuDoRNet is 2.5-5dB lower than SC-DuDoRNet in terms of PSNR with the same input. The 2<sup>nd</sup> sub-table compares DuDoUniNeXt with some multi-contrast (MC) reconstruction methods by using paired (T2w, PD) from IXI to simulate two different combinations of target and reference. Adding an LQ  $I_{ref}$ , the reconstruction is boosted by 4-7dB in PSNR and further by another 2-3dB for an HQ  $I_{ref}$ . For comparison, MTrans and MC-DuDoRNet still lag behind

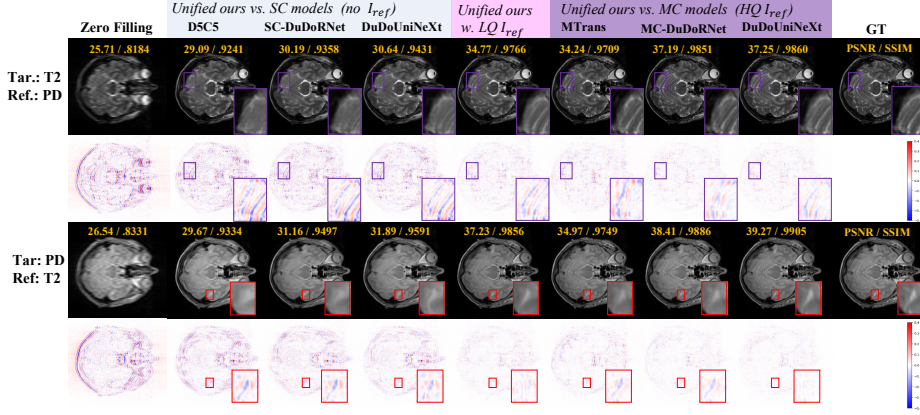


**Fig. 4.** Qualitative comparisons of  $5 \times$  undersampled T2 and PD reconstruction under different  $I_{ref}$  conditions. Corresponding error maps are illustrated in BWR colormaps.

SC-models with an LQ  $I_{ref}$  as input and show a lower PSNR and SSIM than our DuDoUniNeXt under the specific fully-sampled reference-guided scenario.

Qualitative comparison of various T2 and PD reconstructions under different conditions of  $I_{ref}$  is shown in Fig. 4. We also zoom in two typical regions: a highly structural region of the T2w image in **violet** and an isolated small tissue of the PD image in **red**. Our model handles both structures and details better than existing SC and MC models.

**Ablation studies** We validate the effectiveness of each novel component: AdaC2F, unified learning scheme, PaSS, XBB, and training scheme, and show the results in Table 2. (1) We demonstrate the superiority of AdaC2F by substituting it with existing feature fusion strategies: Max[2], HeMIS[12], DFUM[40] and a reverse-version of ours, AdaF2C. (2) We verify our dual-domain learning schemes with different image and k-space network layouts and unification schemes. (3) We verify our PaSS by adjusting the  $CB_i$ 's with completely shared or completely distinct weights. (4) We substitute XBB with existing DRDN [43] and RSTB [22,16,26] as building blocks. More studies on domain-specificity and hybrid strategy are provided in the supplement. (5) We train existing MC models under our training scheme to show the training scheme is not the only reason for our performance gain. The superiority of DuDoUniNeXt's components is consistent.

## 4 Conclusion

We propose a novel approach for unified single-contrast and multi-contrast MRI reconstruction using a dual-domain network and an efficient CNN-ViT hybrid backbone. The experimental results on IXI and FastMRI demonstrate the superior adaptability and performance of DuDoUniNeXt against single-purpose SoTA

PSNR(dB)/SSIM(%)		HQ $I_{ref}$	LQ $I_{ref}$	Missing $I_{ref}$	PSNR(dB)/SSIM(%)		HQ $I_{ref}$	LQ $I_{ref}$	Missing $I_{ref}$
Fusion	Max [2]	39.59/99.01	37.51/98.58	32.10/96.00	Shallow	Shared	39.13/98.93	37.18/98.50	32.04/95.94
	HeMIS [12]	39.60/99.01	37.59/98.59	32.08/95.97	Feature	Distinct	39.54/99.01	37.54/98.58	32.09/95.99
	DFUM [40]	39.61/98.87	37.49/98.55	32.11/95.98	Extractor	PaSS (ours)	<b>39.63/99.03</b>	<b>37.68/98.63</b>	<b>32.39/96.19</b>
	AdaF2C	39.33/98.96	37.46/98.62	32.22/95.88	Backbone	DRDN [43]	38.87/98.86	36.56/98.33	31.64/95.87
	AdaC2F (ours)	<b>39.63/99.03</b>	<b>37.68/98.63</b>	<b>32.39/96.19</b>	Building	RSTB [22,16,26]	39.13/98.90	37.12/98.58	31.95/96.01
Dual-domain	Unil-UniK	38.37/98.69	36.79/98.21	30.91/94.68	Block	XBB (ours)	<b>39.63/99.03</b>	<b>37.68/98.63</b>	<b>32.39/96.19</b>
Unified	UniK-Unil	39.24/98.96	37.63/98.61	31.85/96.79	Training	DuDoRNet w. TS	39.01/98.89	33.93/95.12	31.55/95.38
Learning	Unil-K	39.09/98.83	37.61/98.50	31.36/95.14	Scheme	MTrans w. TS	35.05/97.50	33.03/96.40	28.16/91.04
	K-Unil (ours)	<b>39.63/99.03</b>	<b>37.68/98.63</b>	<b>32.39/96.19</b>		Ours	<b>39.63/99.03</b>	<b>37.68/98.63</b>	<b>32.39/96.19</b>

**Table 2.** Ablation studies. We use T2w images under different conditions as  $I_{ref}$  to guide  $5\times$  undersampled PD reconstruction. The **best** results are colored **red**.

models. The current study is based on the single-coiled images for a proof-of-concept and we will adapt it to multi-coil datasets in the future.

## References

1. Ixi dataset. [brain-development.org/ixi-dataset](http://brain-development.org/ixi-dataset), CC BY-SA 3.0 license
2. Chartsias, A., Joyce, T., Giuffrida, M.V., Tsaftaris, S.A.: Multimodal mr synthesis via modality-invariant latent representation. *IEEE Transactions on Medical Imaging* (2018)
3. Cheng, J., Wang, H., Ying, L., et al.: Model learning: Primal dual networks for fast mr imaging. In: *MICCAI* (2019)
4. Chung, H., Ye, J.C.: Score-based diffusion models for accelerated mri. *Medical Image Analysis* p. 102479 (2022)
5. Dar, S.U., Yurt, M., Shahdloo, M., et al.: Prior-guided image reconstruction for accelerated multi-contrast mri via generative adversarial networks. *IEEE Journal of Selected Topics in Signal Processing* **14**(6), 1072–1087 (2020)
6. Eo, T., Jun, Y., Kim, T., et al.: Kiki-net: cross-domain convolutional neural networks for reconstructing undersampled magnetic resonance images. *Magnetic resonance in medicine* **80**(5), 2188–2201 (2018)
7. Feng, C.M., Yan, Y., et al.: Multi-modal transformer for accelerated mr imaging. *IEEE Transactions on Medical Imaging* (2022)
8. Gao, Z., Zhou, S.K.: Rethinking dual-domain undersampled mri reconstruction: domain-specific design from the perspective of the receptive field. In: *ISBI* (2024)
9. Gungor, A., Dar, S.U., et al.: Adaptive diffusion priors for accelerated mri reconstruction. *Medical Image Analysis* p. 102872 (2023)
10. Guo, P., Mei, Y., Zhou, J., Jiang, S., Patel, V.M.: Reconformer: Accelerated mri reconstruction using recurrent transformer. *IEEE Transactions on Medical Imaging* pp. 1–1 (2023)
11. Guo, P., Valanarasu, J.M.J., Wang, P., et al.: Over-and-under complete convolutional rnn for mri reconstruction. In: *MICCAI* (2021)
12. Havaei, M., Guizard, N., Chapados, N., Bengio, Y.: Hemis: Hetero-modal image segmentation. In: *MICCAI* (2016)
13. Herrmann, J., Keller, G., Gassenmaier, S., Nickel, et al.: Feasibility of an accelerated 2d-multi-contrast knee mri protocol using deep-learning image reconstruction: a prospective intraindividual comparison with a standard mri protocol. *European Radiology* **32** (04 2022)
14. Hu, J., Shen, L., Sun, G.: Squeeze-and-excitation networks. In: *CVPR* (2018)
15. Huang, J., Aviles-Rivero, A., Schönlieb, C.B., Yang, G.: Cdiffmr: Can we replace the gaussian noise with k-space undersampling for fast mri? (2023)
16. Huang, J., Fang, Y., Wu, Y., Wu, H., Gao, Z., Li, Y., Del Ser, J., Xia, J., Yang, G.: Swin transformer for fast mri. *Neurocomputing* **493**, 281–304 (2022)
17. Huang, J., Xing, X., Gao, Z., Yang, G.: Swin deformable attention u-net transformer (sdaut) for explainable fast mri. In: *MICCAI* (2022)
18. Kingma, D.P., Ba, J.: Adam: A method for stochastic optimization. *arXiv preprint arXiv:1412.6980* (2014)
19. Knoll, F., Zbontar, J., Sriram, A., et al.: fastmri: A publicly available raw k-space and dicom dataset of knee images for accelerated mr image reconstruction using machine learning. *Radiology: Artificial Intelligence* **2**(1), e190007 (2020)
20. Korkmaz, Y., Cukur, T., Patel, V.: Self-supervised mri reconstruction with unrolled diffusion models (2023)
21. Korkmaz, Y., Dar, S.U., Yurt, M., Özbey, M., Cukur, T.: Unsupervised mri reconstruction via zero-shot learned adversarial transformers. *IEEE Transactions on Medical Imaging* **41**(7), 1747–1763 (2022)

22. Liang, J., Cao, J., Sun, G., Zhang, K., Van Gool, L., Timofte, R.: Swinir: Image restoration using swin transformer. In: WACV (2021)
23. Liu, X., Wang, J., Jin, J., et al.: Deep unregistered multi-contrast mri reconstruction. *Magnetic Resonance Imaging* **81**, 33–41 (2021)
24. Liu, X., Wang, J., Sun, H., et al.: On the regularization of feature fusion and mapping for fast mr multi-contrast imaging via iterative networks. *Magnetic resonance imaging* **77**, 159–168 (2021)
25. Liu, Z., Lin, Y., Cao, Y., Hu, H., Wei, Y., Zhang, Z., Lin, S., Guo, B.: Swin transformer: Hierarchical vision transformer using shifted windows. In: ICCV (2021)
26. Lyu, J., Sui, B., Wang, C., et al.: Dudocaf: Dual-domain cross-attention fusion with recurrent transformer for fast multi-contrast mr imaging. In: MICCAI (2022)
27. Pan, J., Shit, S., et al.: Global k-space interpolation for dynamic mri reconstruction using masked image modeling. MICCAI (2023)
28. Park, N., Kim, S.: How do vision transformers work? In: ICLR (2022)
29. Peng, C., Guo, P., Zhou, S.K., Patel, V.M., Chellappa, R.: Towards performant and reliable undersampled mr reconstruction via diffusion model sampling. MICCAI (2022)
30. Peng, C., Lin, W.A., Chellappa, R., et al.: Towards multi-sequence mr image recovery from undersampled k-space data. In: MIDL (2020)
31. Qin, C., Schlemper, J., et al.: Convolutional recurrent neural networks for dynamic mr image reconstruction. *IEEE transactions on medical imaging* **38**(1), 280–290 (2018)
32. Quan, T.M., Nguyen-Duc, T., Jeong, W.K.: Compressed sensing mri reconstruction using a generative adversarial network with a cyclic loss. *IEEE transactions on medical imaging* **37**(6), 1488–1497 (2018)
33. Schlemper, J., Caballero, J., Hajnal, J.V., othersl: A deep cascade of convolutional neural networks for mr image reconstruction. In: IPMI (2017)
34. Wang, S., Su, Z., Ying, L., Peng, X., Zhu, S., Liang, F., Feng, D., Liang, D.: Accelerating magnetic resonance imaging via deep learning. In: ISBI (2016)
35. Wang, S., Zhao, T., Huang, N., et al.: Feasibility of multi-contrast mr imaging via deep learning. *ISMRM* (2017)
36. Xiang, L., Chen, Y., Chang, W., Zhan, Y., Lin, W., Wang, Q., Shen, D.: Ultra-fast t2-weighted mr reconstruction using complementary t1-weighted information. In: MICCAI 2018 (2018)
37. Xuan, K., Xiang, L., Huang, X., Zhang, L., Liao, S., Shen, D., Wang, Q.: Multi-modal mri reconstruction assisted with spatial alignment network. *IEEE Transactions on Medical Imaging* **41**(9), 2499–2509 (2022)
38. Yang, G., Yu, S., Dong, H., Slabaugh, G., Dragotti, P.L., et al.: Dagan: deep de-aliasing generative adversarial networks for fast compressed sensing mri reconstruction. *IEEE transactions on medical imaging* **37**(6), 1310–1321 (2017)
39. Zbontar, J., Knoll, F., Sriram, A., et al.: fastmri: An open dataset and benchmarks for accelerated MRI. *CoRR* **abs/1811.08839** (2018)
40. Zhang, Y., Peng, C., Wang, Q., Song, D., Li, K., Zhou, S.K.: Unified multi-modal image synthesis for missing modality imputation. *arXiv preprint arXiv:2304.05340* (2023)
41. Zhang, Z., Romero, A., Muckley, M.J., et al.: Reducing uncertainty in undersampled mri reconstruction with active acquisition. In: CVPR (2019)
42. Zhou, B., Dey, N., Schlemper, J., et al.: Dsformer: a dual-domain self-supervised transformer for accelerated multi-contrast mri reconstruction. In: WACV (2023)
43. Zhou, B., Zhou, S.K.: Dudornet: learning a dual-domain recurrent network for fast mri reconstruction with deep t1 prior. In: CVPR (2020)